Journal of Advanced Engineering Trends
ISSN : 2682 - 2091

Vol. 44, No. 1, January 2025

Development and Optimization of a Catalyzed Biodiesel Production Process from LTW

Moatasem Kamel[1,*], Mohsen A. Hashem[1], Ibrahim Ashour[1]

[1] *Chemical Engineering Dep., Faculty of Engineering, Minia University, Minia, Egypt*
** Corresponding author(s) E-mail: moatasem.m.kamel@mu.edu.eg*

ARTICLE INFO

Article history:
Received: 16 October 2024
Accepted: 9 December 2024
Online: 1 March 2025

Keywords:
Limed fleshing waste (LFW),
Waste valorization,
Biodiesel Production,
Response Surface Methodology (RSM).

ABSTRACT

Due to the generation of fat-rich residues from the leather industry, these fat-rich residues are considered a promising feedstock for waste valorization into biofuel applications. Limed flashing waste (LFW), collected from Badr City, Egypt, was subjected to different multi-purpose pretreatment steps, including delimiting, drying, chopping, Soxhlet extraction, and degumming to recover oil. The recovered oil was then transesterified with methanol using commercial CaO as a catalyst. Multi-variable regression modeling was applied to optimize the triglyceride conversion into biodiesel. The optimized reaction conversion yielded a conversion of 97.74% achieved under a methanol-to-oil ratio of 8.93:1, 5.74% w/w catalyst loading, 63.4°C reaction temperature, agitation speed at 300 rpm, and 3 hours of reaction time. GC-MS and FT-IR analysis both confirm the conversion of LFW into biodiesel, highlighting its suitability and feasibility as an alternative source for sustainable energy. It was demonstrated that LFW produced from the leather industry, whose handling and discarding are challenging, can be converted into biofuel. Thereby contributing to waste management and energy demands.

1. Introduction

Countries are looking for sustainable and cost-effective energy sources to enhance their energy security, support economic sustainability, reduce greenhouse gas emissions, and avoid potential depletion of petroleum-based fuels [1, 2]. Biodiesel is characterized by its low sulfur, carbon, and aromatic compounds. Biodiesel also has higher cetane number and higher efficiency when compared to conventional diesel [3, 4]. Biodiesel production from human food and edible oil has led to certain ethical and economic concern since it could affect the human right to have enough food [5]. Recent research focuses on non-edible oils, e.g., Karanja, jatropha, and waste cocking oils, as a raw material for waste-derived biodiesel synthesis [6]. Non-edible oil offers several advantages against other feedstocks owing to their cost, availability, reduced competition with food production, and high oil content [6]. Also, their valorization will minimize waste and contribute to a more circular economy since this approach not only supports energy security but also minimizes environmental impacts [7]. One of the most premising non-edible feedstocks for biofuel synthesis is the leather fleshing waste (LFW), which is a type of waste generated from hides and is treated with lime and sodium sulfide during the pre-tanning stage. LFW requires proper treatment before disposal to reduce its effect on the environment [8]. Traditional treatments of leather fleshing waste include incineration or landfilling, which have dangerous environmental drawbacks [9]. Incineration leads to the release of greenhouse gases (GHGs) such as CO_2 and CH_4 and the production of harmful air pollutants, thereby contributing to climate change [10]. On the other hand, landfilling may result in the release of toxic chemicals into the soil, thereby affecting water quality [11].

The Egyptian government has identified the leather industry as a crucial sector for economic development by increasing exports. As a part of Egypt Vison 2030, the country is investing in the modernization of the leather industry and maintaining sustainability by developing an integrated industrial cluster known as Robbiki Leather City, which is not only a major national project for Egypt but also the largest and most unique eco-industrial leather hub in the Middle East and Africa. Because so many leftovers and byproducts are produced during the tanning process, the leathercraft sector is frequently known for producing more waste than products. An estimated 850 kg of waste are produced for every ton of raw hide. About 56-60% of this waste is fleshing waste [12]. This waste not only poses environmental challenges but also represents a potential resource for energy recovery and material reuse.

Most of the solid waste generated from tanneries is produced during the fleshing and trimming stages; these stages generate abundant fat-rich residues that hold the potential for valorization through conversion into biodiesel. The pre-fleshing stage removes unwanted tissue and ensures optimal chemical penetration for better leather quality [13]. Although leather industry waste contains high fat content, they remain underutilized, and the industry lacks efficient methods for fat recovery and use to minimize the environmental impact of leather waste disposal and produce bio-based fuel, thereby contributing to a more sustainable future [14].

Biodiesel production feasibility depends on two factors: feedstock competition with food production and cost effectiveness [8]. Since the feedstock cost of accounts for about 70-95% of the overall cost, therefore, finding a low-cost and abundant feedstock

can reduce production costs [15]. In view of this, this study aims to develop an extraction method to extract fats from a low-cost, environmentally polluting, and underutilized waste stream (LFW). Optimize factors influencing the biodiesel production using response surface methodology (RSM) by predicting the optimal parameters for maximum response (yield). Characterize the properties of the produced biodiesel to assess its quality and suitability as a biofuel.

2. Materials and Methods

2.1. Materials

LFW was collected from El Liethy tannery at El-Robbiki city cluster, Badr city, Cairo, Egypt. Methanol (99.8%) and hexane (99%) were purchased from Piochem, 6th of October City, Giza, Egypt. Also, pure calcium oxide powder was obtained from MM Egypt Company, Tower of Trees, Al-Manshiyeh St. Clock Sq. Talbiya Faisal – Giza, Egypt. All other chemicals used through this study were of analytical grade.

2.2. Methods

2.2.1 LFW Pretreatment and Oil Extraction:

LFW underwent multiple washes with water to eliminate impurities, e.g., dirt, blood, and salts. The pH of the waste was neutralized by soaking in a 1% (w/w) formic acid solution for one hour, then heated for 1 hour at 105 °C to eliminate water, and finally, it was mechanically chopped into smaller particle sizes, optimizing it for downstream processing into biodiesel.

The Soxhlet apparatus was used for the extraction of fats from LFW. As figure 1 shows, the chopped waste was charged within a thimble, which resides between the condenser at the top and the 500-mL round-bottom flask containing the extracting solvent (n-hexane). During the extraction process, the solvent (300-mL for 250 g of waste) vaporizes due to heating, and the vapor rises up through the tube and then condenses in the water-cooled condenser. The condensed solvent then dripped onto the chopped LFW in the thimble, thereby extracting the required fats. The siphoning mechanism of the Soxhlet allows for a continuous cycle of returning the solvent-oil mixture to the round bottom flask, which is reheated again until the oil is extracted completely. The subsequent step was solvent-oil separation using a rotary evaporator, which separates the oil and hexane based on the difference in boiling points. The extracted oil yield of the was determined using the following formula:

$$\text{Oil Yield } (\%) = \frac{\text{Total weight of the dry oil}}{\text{Total weight of flesh sample}} * 100 \qquad (1)$$

2.2.2 Recovered oil Pretreatment:

Following oil extraction, the extracted oil was degummed to eliminate phospholipids, a class of impurities that could hinder downstream biodiesel production. A glass reactor, heated and stirred by a hot plate magnetic stirrer, was employed for the purification process. The crude oil was first heated to 70 °C. Chemical degumming was carried out at 200 rpm using 2% v/v orthophosphoric acid/LFW oil and 3% v/v distilled water/LFW oil. This means that for every 100 mL of LFW oil, 2 mL of orthophosphoric acid is mixed with 3 mL of distilled water to create the degumming solution, which is then mixed with the heated oil. These percentages ensure that the amounts of acid and water are proportionate to the amount of oil without using excess acid and/or water [8]. After degumming for an hour, the mixture is cooled down to room temperature and centrifuged at 800 rpm for about 20 minutes to separate the gums and any other impurities from the oil. After that, the degummed oil was heated to 105°C to ensure the oil does not contain any residual water.

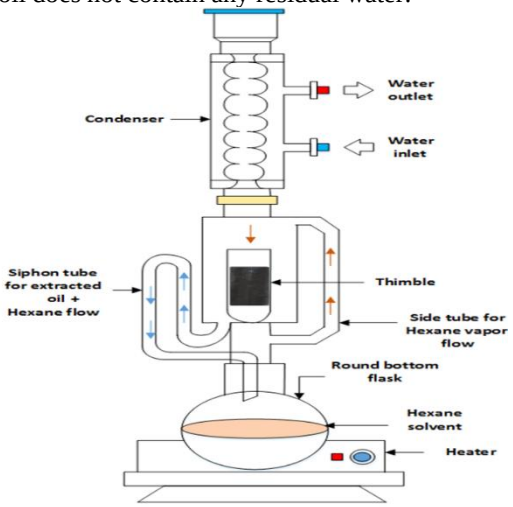

Figure 1: **Soxhlet extraction process**

2.3. Evaluation of thermal and physicochemical properties

The thermal and physicochemical properties of the LFW oil (pre- and post-degumming) and the produced biodiesel were evaluated according to the ASTM standards [16]. The evaluation took place at the Energy and Environment Lab, Sepuluh Nopember Institute of Technology, Surabaya, Indonesia. The following physicochemical parameters were investigated: high heat value, density, kinematic viscosity, acid value, iodine number, cetane number, saponification number, and free fatty acid content [17].

2.4. Biodiesel Production

Biodiesel was produced from LFW oil through the transesterification process. This process involves the following steps: mixing the catalyst and the alcohol, reaction, product separation, washing, drying, and filtration. The steps involved in the production of fatty acid methyl esters (FAMEs), via methanolysis reaction, are shown schematically in figure 2.

LFW oil was heated in a laboratory stirred tank reactor to 120°C for 1 hour to eliminate any residual water. Methanol was then mixed with a heterogenous CaO catalyst and mixed with the dried oil. Various parameters were investigated to optimize the production process. These parameters include reaction time, temperature, catalyst loading, and MeOH-to-oil molar ratio. The reaction mixture was then agitated at 300 rpm for a predetermined period of time. The product mixture was then allowed to settle, resulting in the formation of three distinct phases: the biodiesel phase, glycerol phase, and catalyst phase. The glycerin separation step during FAME production is shown in figure 3. Following this step, the separated FAME was washed, dried with 0.5 g of Na_2SO_4 for every 100 mL of biodiesel, and filtered using a fine filter paper to remove any residual solid impurities.

Transesterification efficiency was evaluated by calculating biodiesel yield using the following formula:

$$\text{Biodiesel Yield (\%)} = \frac{\text{Weight of methyl esters}}{\text{Weight of oil sample}} * 100 \qquad (2)$$

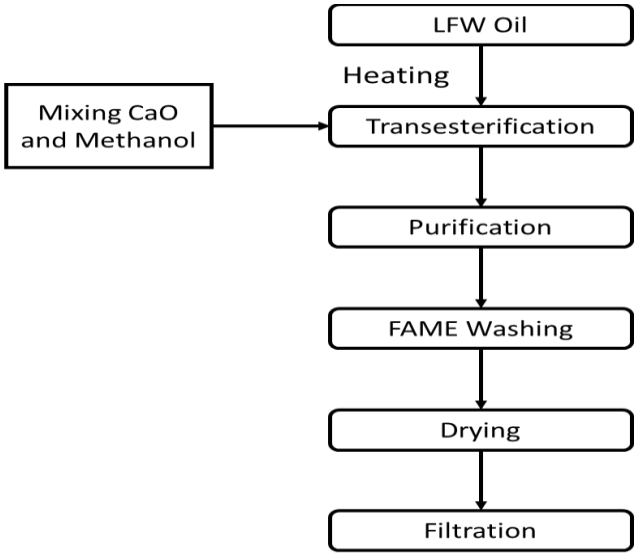

Figure 2: FAME production via Transesterification

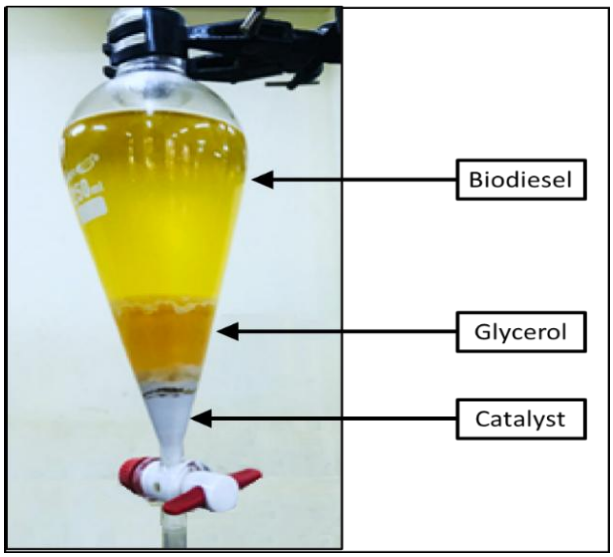

Figure 3: FAME and Glycerin separation step

2.5. RSM Statistical Optimization:

RSM analysis was used as a statistical tool for analyzing the key reaction parameters and optimizing biodiesel yield using Design-Expert® 13.0.5.0 software. The experimental data was optimized via analysis of variance (ANOVA) using Box Behnken Design (BBD), a widely used RSM design used for statistical analysis and design of experiments [18]. BBD determines the optimal number of experimental runs (n) based on the following formula:

$$n = 2K(K-1) + C_0 \qquad (3)$$

where K denotes the reaction variables numbers taken into account (K = 3) and C_0 represents the number of center points (C_0 = 5) [17].

Testing the effect of methanol-to-oil ratio (A), catalyst dosage (B), and temperature (C) required a total of 17 experimental runs, enabling identification of the optimal parameter values for maximum yield. Factors levels are shown in Table 1 in terms of coded symbols and levels. These ranges were adopted from [8, 17], where similar experimental conditions were applied for biodiesel production from different animal fats. Table 2 lists the values of the input parameters for each run based on the BBD along with their corresponding yield.

Table 1: Process parameters ranges and levels.

Factor	Unit	Symbol Coded	Range and Level		
			-1	0	1
Methanol to oil ratio	-	A	3	6	9
Amount of catalyst	%	B	2	4	6
Temperature	70 °C	C	50	60	70

Table 2: Experimental run design derived using RSM

Run	A: Molar Ratio	B: Catalyst Loading	C: Temperature	Exp. Yield	Pred. Yield	Residual
		%	°C	%	%	
1	6	4	60	88.71	88.10	0.6100
2	6	4	60	88.47	88.10	0.3700
3	6	2	50	53.12	53.17	-0.0488
4	6	4	60	88.04	88.10	-0.0600
5	6	6	50	63.3	63.15	0.1538
6	9	4	70	85.08	84.99	0.0938
7	3	6	60	85.54	85.60	-0.0600
8	6	4	60	87.24	88.10	-0.8600
9	6	6	70	80.32	80.27	0.0487
10	3	4	50	52.78	52.87	-0.0938
11	9	4	50	55.34	55.35	-0.0112
12	9	6	60	96.38	96.52	-0.1425
13	3	4	70	63.67	63.66	0.0112
14	9	2	60	90.67	90.61	0.0600
15	6	2	70	76.31	76.46	-0.1538
16	3	2	60	77.87	77.73	0.1425
17	6	4	60	88.04	88.10	-0.0600

3. Results and discussions

3.1. Extracted Oil Characterization

Assessment of the degumming process was evaluated by measuring and comparing the physicochemical properties of the extracted oil (pre- and post-degumming). The measured properties are summarized in Table 3. The density of the degummed oil was reduced from 913 to 902 kg/m^3 due to the removal of phospholipids and other impurities during the degumming process. These compounds typically contribute to the overall density of the oil because they contain heavy molecules. Kinematic viscosity also decreased from 41.1 to 29.32 mm^2/s. This reduction is beneficial for biodiesel production since lower viscosity oils enhance process efficiency [19]. Acid value was also reduced to 2.74 mg NaOH/g due to the removal of phospholipids, which may hydrolyze into free fatty acids (FFAs), which increases the acid value, and the use of acid catalysts, which contribute to the neutralization of the FFAs present [20]. Degumming causes a slight increase in the higher heating value (HHV) since phospholipids have a lower calorific

value compared to the triglycerides (the main component of oils and fats) [21]. FFA content decreased from 1.68 to 1.37% due to the addition of an acid catalyst during the degumming process, which causes the phospholipids to form gum, which is then separated from the oil. Also, the saponification value of the fleshing oil was decreased after degumming from 197.8 to 180.2 mg KOH/g due to the removal of phospholipids. Phospholipids have higher saponification value due to the presence of multiple fatty acid chains that can be easily saponified. On degumming, the oil became richer in triglycerides, which have a lower saponification value due to the longer fatty acid chain present [22].

Table 3: Comparison of the Physicochemical Characteristics of both untreated and treated fleshing oil

Parameter	Unit	Untreated Oil	Treated Oil
Density	**Kg/m^3**	**913**	**902**
Kinematic Viscosity	**mm^2/s**	**41.1**	**29.32**
Acid Value	**mg NaOH/g**	**3.36**	**2.74**
HHV	**MJ/kg**	**43.24**	**43.86**
Iodine value	**g I_2/100g**	**78**	**64.5**
FFA	**%**	**1.68**	**1.37**
Saponification Value	**mg KOH/g**	**197.8**	**180.2**

3.2. Transesterification Reaction time optimization:

The effect of time on converting degummed fleshing oil into FAME was studied and reported in figure 4. It was indicated that the conversion reaches the maximum yield within 3 hours, achieving 88% of the complete conversion, which indicates that the reaction kinetics are favorable under the specified conditions (alcohol to oil ratio = 6:1, dose of catalyst = 4%, and temperature of 60 °C). Extending the reaction time to 5 hours led to a small increase in the conversion yield, to 90%, indicating that the reaction reaches equilibrium. Considering these results, a reaction time of 3 hours had been selected for all runs.

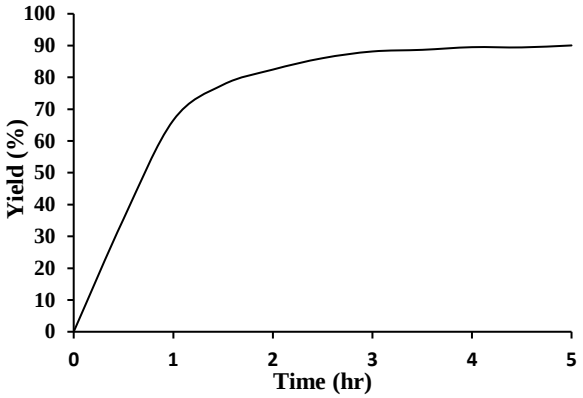

Figure 4: **Reaction time optimization**

3.3. ANOVA Analysis:

Following the procedures described in Section 2.4, a methanolysis reaction was conducted to convert the extracted and degummed LFW oil into FAME. Regression and graphical analysis were carried out using design expert software as outlined earlier. The experimental results were fitted to various models to investigate how the reaction parameters affect the percentage yield.

After finishing the experimental runs and recording the calculated yield as the response, the data fitting analysis was evaluated and presented in Table 4 for linear, two-factor interaction (2F1), quadratic, and cubic models. Based on the sequential model sum of squares, the optimal model is the one with significant additional terms and is not aliased. A model is said to be aliased when the estimate of an effect is influenced by one or more effect, usually higher-order interactions. The optimal model selection was based on the standard deviation, R^2, adjusted R^2, predicted R^2, and predicted residual error sum of squares (PRESS) values of the models. The quadratic model best fitted the experimental data as it demonstrated the highest R^2 (0.9996), adjusted R^2 (0.9991), and predicted R^2 (0.9988). The rule of thumb suggests a difference of less than 0.2 between predicted R^2 and adjusted R^2 values, which is met in this case (difference of 0.0003). Also, the quadratic model, compared to other models, has the lowest standard deviation (0.4430), further supporting the applicability of the model to the data.

Table 4: Comparison of Model Fit Statistics for Different Polynomial Models

Source	Std. Dev.	R^2	Adjusted R^2	Predicted R^2	PRESS
Linear	12.76	0.3607	0.2132	-0.1803	3910.85
2FI	14.21	0.3907	0.0251	-1.4744	8198.52
Quadratic	**0.4430**	**0.9996**	**0.9991**	**0.9988**	**3.84**
Cubic	0.5603	0.9996	0.9985		

To further investigate the relevance of the quadratic model, the p-value of the model and its individual terms were evaluated. A lower p-value suggests that the model is significant, which means that it is unlikely to have occurred by chance. The quadratic model was statistically significant since p-value < 0.0001, which is less than 0.05. Also, the individual model terms A, B, C, AC, BC, A^2, B^2, and C^2 are significant contributors to the model, as their p-values < 0.05. Conversely, any other terms with a p-value greater than 0.05 are considered to be non-significant contributors to the model, and their effect can be ignored. The lack of fit F-value of 0.12 indicated that it fits the data well since it does not differ from the pure error (p-value of 94.05%). These results ensure that the quadratic model is the most suitable model for the data. The final proposed model that correlates the required response to the key affecting parameters, expressed in terms of the coded factors, is presented in equation 4 along with the ANOVA in table 5.

$$\begin{aligned}\text{Yield } \% = {} & 88.10 + 5.95\,A + 3.45\,B + 10.11\,C \\ & - 0.4900\,AB + 4.71\,AC - 1.54\,BC \\ & - 2.26\,A^2 + 1.78\,B^2 - 21.62\,C^2\end{aligned} \quad (4)$$

Table 6 presents the fit statistics of the proposed quadratic model. The adequacy precision ratio of 128.4798 exceeds the desirable value of 4. This high signal-to-noise ratio means that the model had successfully identified the key interaction parameters affecting the response (yield) within the defined experimental conditions. Figure 5 presents the quadratic model accuracy across the specified conditions. The diagonal represents the perfect prediction. As seen, almost all the data typically fits the diagonal, indicating a high level of agreement and high accuracy between the actual calculated data and the data predicted by the model.

Table 5: ANOVA table for the quadratic model.

Source	Sum of Squares	df	Mean Square	F-value	p-value	significance
Model	3311.95	9	367.99	1875.51	< 0.0001	significant
A-Molar Ratio	283.34	1	283.34	1444.05	< 0.0001	
B-Catalyst Loading	95.01	1	95.01	484.24	< 0.0001	
C-Temperature	816.89	1	816.89	4163.32	< 0.0001	
AB	0.9604	1	0.9604	4.89	0.0626	
AC	88.83	1	88.83	452.73	< 0.0001	
BC	9.52	1	9.52	48.51	0.0002	
A^2	21.6	1	21.6	110.09	< 0.0001	
B^2	13.34	1	13.34	67.99	< 0.0001	
C^2	1967.65	1	1967.65	10028.24	< 0.0001	
Residual	1.37	7	0.1962			
Lack of Fit	0.1177	3	0.0392	0.1249	0.9405	not significant
Pure Error	1.26	4	0.3139			
Cor Total	3313.33	16				

Table 6: Fit Statics

Std. Dev.	0.4430	R^2	0.9996
Mean	77.70	Adjusted R^2	0.9991
C.V. %	0.5701	Predicted R^2	0.9988
		Adeq Precision	128.4798

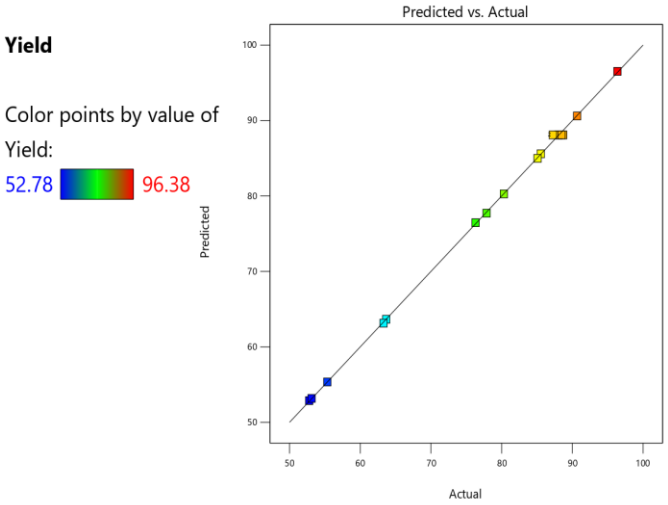

Figure 5: Quadratic model prediction of conversion versus actual conversion

3.4. Influence of Interactions Between Process Variables on Biodiesel Yield:

In this study, 3D response plots were applied to show how the interaction between two different key parameters affects biodiesel yield while maintaining the third parameter fixed. The description of each individual plot will be discussed in the following sections.

(a) Biodiesel Yield: The Impact of Molar Ratio and Catalyst

Figure 6 shows a 3D response curve that illustrates the interaction between alcohol to oil ratio and amount of catalyst used on FAME conversion, with the reaction temperature, time, and stirring speed held constant at 60 °C, 3 hours, and 300 rpm, respectively. The figure shows that the response increases with increasing molar ratio from 1:3 to 1:9. This trend is consistent with the stoichiometric requirement of the transesterification reaction, that methanol availability pushes the reaction equilibrium towards complete conversion of triglycerides to FAME [23]. Similarly, increasing the catalyst dosage from 2 to 6 wt% increases the conversion yield, reaching its maximum value at 6 wt%. This is because increasing the amount of CaO catalyst facilitates the transesterification reaction owing to the enhanced accessibility of active sites on the catalyst. The optimum biodiesel yield predicted was 96.38% at a molar ratio of 9:1 methanol to oil and a catalyst weight of 6 wt%.

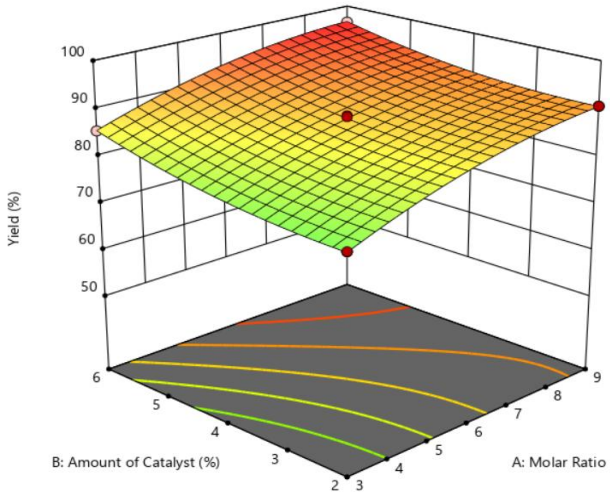

Figure 6: Interactive Effects of methanol-to-oil ratio and catalyst dosage on biodiesel yield, while temperature remain constant at 60°C

(b) Biodiesel Yield: The Impact of Temperature and Molar Ratio

Figure 7 illustrates how the interaction between reaction temperature and alcohol to oil molar ratio affects the required yield, with catalyst loading, agitation speed, and reaction time fixed at 4 wt%, 300 rpm, and 3 hours, respectively. The response surface plot shows that higher temperatures (typically from 50 to 64 °C) enhance the conversion of triglycerides to FAMEs due to the enhanced kinetic energy, as increasing the reaction temperature increases the kinetic energy of both reactants, the alcohol and triglycerides. This results in more frequent and energetic collisions, thereby accelerating and facilitating the reaction rate. Also, increasing the reaction temperature helps break the triglyceride bonds, which promotes their conversion to FAME and glycerol [24]. The behavior of enhanced transesterification reaction rates at elevated temperatures can be explained by the decrease in feedstock oil viscosity at elevated temperatures, which improves the mixing efficiency between the reactants and allows for a better contact between the reactants and the surface of the catalyst, thereby resulting in a more favorable reaction environment. This phenomenon facilitates the conversion of triglycerides to FAME, thereby contributing to an enhanced biodiesel yield. Figure 7 also shows a gradual decrease in the response at temperatures above 64 °C. This can be due to loss of methanol due to evaporation at a temperature exceeding its boiling

point, which reduces the amount of methanol available for the reaction [24, 25].

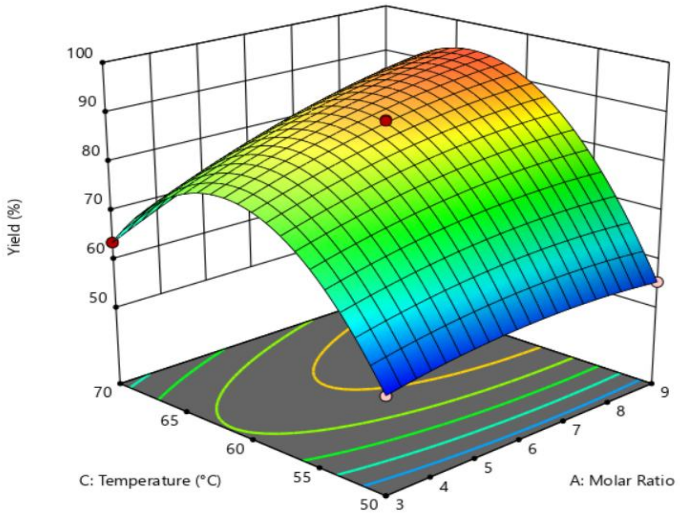

Figure 7: 3D Plot of Temperature and Molar Ratio interplay on biodiesel yield, with amount of catalyst fixed at 4 wt%

(c) Biodiesel Yield: The Impact of Temperature and Catalyst Loading

Figure 8 shows how biodiesel yield is affected by the interplay between reaction temperature and the amount of catalyst used for the transesterification. Stirring speed, reaction time, and molar ratio were held fixed at 300 rpm, 3 hours, and 6:1 molar ratio, respectively. As observed, elevating the reaction temperature from 50 to 64 °C caused the FAME yield to increase due to increased kinetic energy of the reactant molecules which results in an enhanced rate of reaction [24]. The yield then decreases rapidly from 64 to 70 °C due to an imbalance of the methanol stoichiometry due to exceeding the boiling point of methanol.

The figure also shows that the FAME yield increases as the catalyst dose increases. This is likely due to the greater number of reactive sites available at higher concentrations of CaO, which enhances the catalytic activity and thereby results in a higher conversion rate of FAMEs [26].

3.5. Biodiesel Yield Optimization

Optimizing transesterification reaction conditions is important to maximize FAME yield, improving process efficiency, and improving the quality of the produced biodiesel. The quadratic model was used to predict the combination of the process parameters that would achieve the maximum possible yield. From the experimental runs outlined in Table 2, the reaction conditions that yielded the actual maximum FAME yield (96.38%) are as follows: 6 wt% of catalyst, temperature of 60 °C, and 9:1 methanol-to-oil molar ratio. These conditions are also presented in bold font within the same table. Finding the maximum possible biodiesel yield was evaluated through maximizing the desired response (FAME yield) within the design expert software. Figure 9 shows the maximum predicted yield with the corresponding parameter conditions. The quadratic model predicted a 97.72% achievable yield, which closely aligned with the maximum yield achieved experimentally (96.38%). The highest optimal yield predicted by the model was achieved under the following conditions: a molar ratio of 8.93:1 methanol-to-oil, 5.74 wt% of catalyst, and a temperature of 63.4 °C. This strong agreement between the predicted versus the experimental data confirms the model validity and reliability.

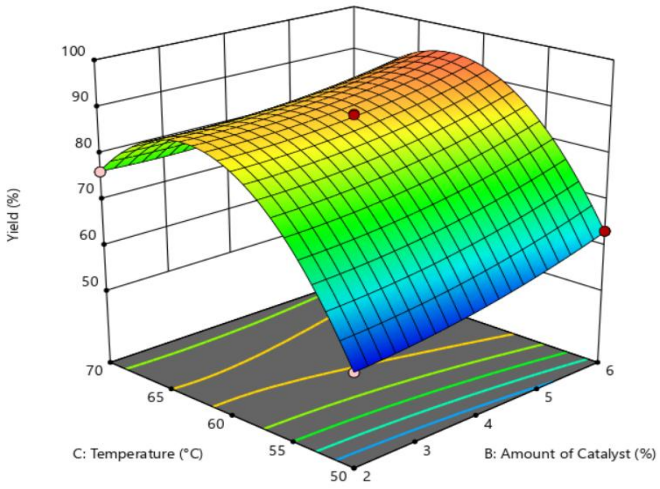

Figure 8: 3D Plot of Temperature and Catalyst Loading interplay on biodiesel yield, with 6:1 methanol/oil ratio)

The predicted process variables suggested by the quadratic model were validated experimentally by testing the transesterification reaction at the optimized A, B, and C values. The FAME yield was determined to be 96.91%. As shown in table 7, the optimal yield reported by the software (97.72%) closely aligns with the experimental yield (96.91%) achieved at the optimized conditions. Further confirming the robustness and accuracy of the model.

Table 7: Comparison of predicted and experimental optimal biodiesel yield

Parameter	Predicted Optimal Conditions	Predicted Yield	Experimental Yield
MeOH/Oil	**8.93:1**		
Catalyst Loading	**5.74 wt%**	**97.72%**	**96.91%**
Temperature	**63.4°C**		

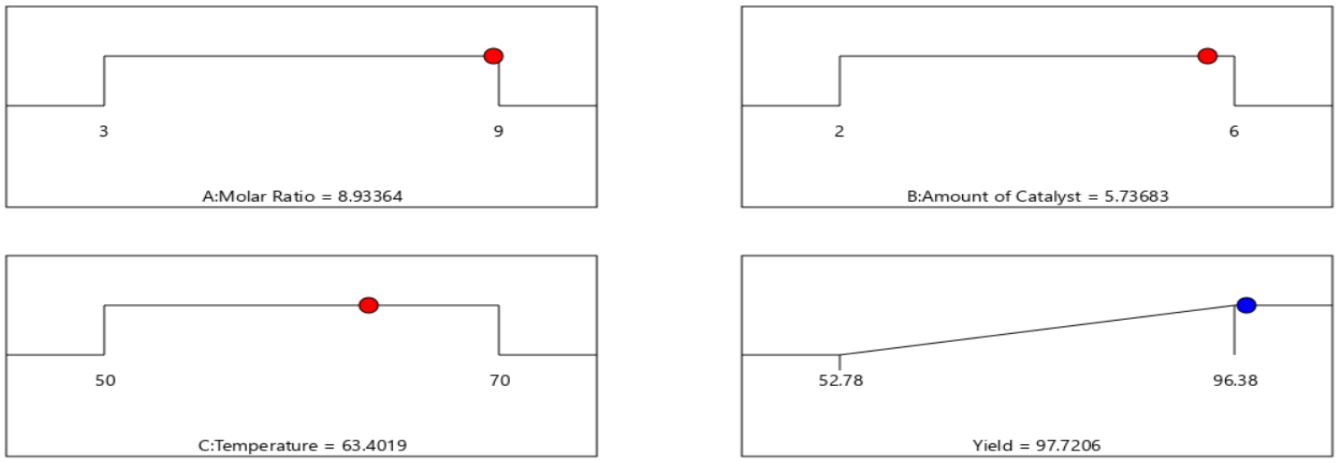

Figure 9: **Fine-Tuning the Process: Optimization Results**

4. Characterization of biodiesel derived Fleshing Waste

4.1. Spectroscopic Infrared Analysis (FT-IR)

The conversion of LFW into FAME is confirmed by observing the stretching and bending of C, H, and O atoms using FT-IR analysis. Figure 10 illustrates the FT-IR spectra of LFW-FAME. The analysis was conducted using a Shimadzu IR Prestige 21 model instrument. In general, biodiesel is always confirmed by the high intensity peaks, which correspond to stretching of C=O and stretching of O–CH_3 [18]. The absorption peak of ester group, a critical component of FAME, was observed at 1744.22 cm^{-1}. This observed peak aligns with the results of Emma et al. [27], who reported the ester group absorption at 1741.72 cm^{-1}. The analysis also confirms the CH stretching peaks at 2925.17 cm^{-1} and 2855.42 cm^{-1} due to the stretching vibrations of the C-H bonds present in methylene (CH_2) and methyl (CH_3) groups, respectively. These absorption peaks align with the peaks reported by Emma et al. [27], who reported similar absorption peaks at 2922.87 cm^{-1} and 2854.56 cm^{-1}. Also, a stretching peak at 1466.67 cm^{-1} was observed in the FT-IR spectra. This peak corresponds to the asymmetric stretching of CH_3 groups.

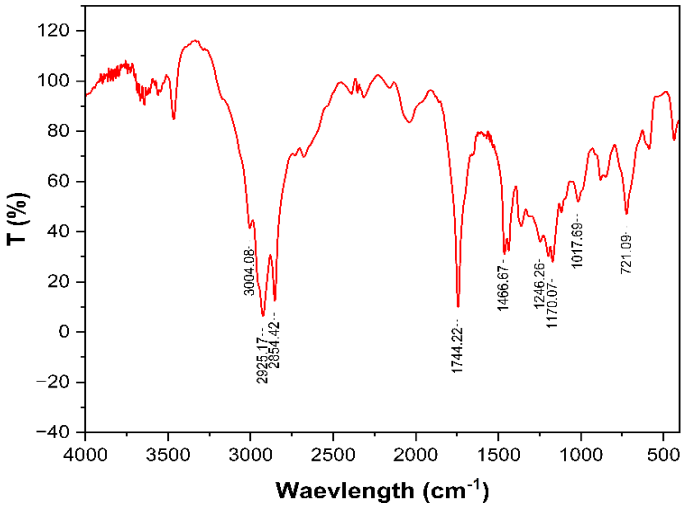

Figure 10: FT-IR Analysis of LFW-Derived Biodiesel

4.2. GC spectral analysis

Comprehensive characterization of the produced FAME was evaluated using GC-MS analysis utilizing GC-MS Shimadzu QP 2010 SE. Methyl oleate and methyl palmitate were reported as predominant fatty acid esters, accounting for 34.11 and 22.284% of the total fatty acid ester composition. Figure 11 illustrates the LFW biodiesel GC spectra, while Table 8 details the composition of the FAME sample. The presence of methyl oleate as the dominant fatty acid ester was reported to improve the cetane number of the biodiesel, therefore contributing to improved engine performance and reduced ignition delay [28].

Table 8: Identified FAMEs in LFW Biodiesel.

Peak No.	Time	Carbon Number	Fatty acid ester	Molecular Formula	Area [%]
1	8.148	C10:0	Methyl decanoate	$C_{11}H_{22}O_2$	0.367
2	11.07	C12:0	Methyl laurate	$C_{13}H_{26}O_2$	2.165
3	13.44	C14:0	Methyl myristate	$C_{15}H_{30}O_2$	2.956
4	15.70	C16:0	Methyl palmitate	$C_{17}H_{34}O_2$	22.284
5	16.48	C16:1	Methyl palmitoleate	$C_{17}H_{33}O_2$	0.794
6	17.75	C18:0	Methyl stearate	$C_{19}H_{38}O_2$	16.954
7	19.42	C18:1	Methyl oleate	$C_{19}H_{36}O_2$	34.111
8	19.65	C18:2	Methyl linoleate	$C_{19}H_{32}O_2$	20.369

4.3. Properties of the FAME Synthesized from LFW

The physicochemical properties of the biodiesel produced from LFW were compared with the established ASTM and EN international standards. Table 9 presents the evaluated properties of the biodiesel along with their respective standard limits. The results reveal that the biodiesel properties fall within the acceptable ranges specified by these international standards. Therefore, highlighting the potential of LFW as an alternative feedstock for biofuel production.

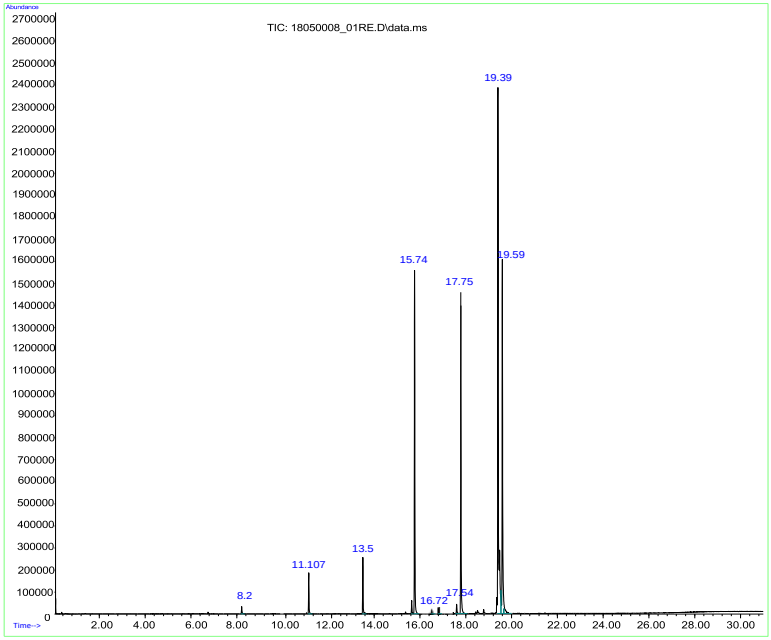

Figure 11: GC spectra of LFW biodiesel

Table 9: Comparison of the Physicochemical Characteristics of the Biodiesel with ASTM & EN Standards

Property	Unit	Test Result	ASTM D 6751-10	EN 14214	Diesel	Test Method
Density	Kg/m^3	864	875-900	860-900	840-860	(EN ISO 3675 & ASTM D 4052)
Kinematic Viscosity	mm^2/s	5.1	1.96-6.0	3.5-5.0	1.9-3.8	ASTM D 445
Acid Value	mg NaOH/g	0.45	≤ 0.8	≤ 0.5	-	ASTM D 664
HHV	MJ/kg	44.1	-	-	43.3-46.7	ASTM D240
Cetane Number	-	64.2	47 minimum	51 minimum		(ASTM D976 & EN ISO 5165)
Iodine Number	g I_2/100g	59	-	120 max.	-	ASTM D 5554

5. Conclusions

In this study, leather fleshing waste had been successfully converted into renewable, high-quality biodiesel, addressing waste management and energy demands. The analysis of the physicochemical properties of the pretreated oil confirmed that the degumming process is a vital step in ensuring the production of high-quality biodiesel. Furthermore, the analysis shows that most of the measured properties comply with the international standards. The GC-MS analysis of the biodiesel samples confirms that LFW could be a potential feedstock for biodiesel synthesis. Successful conversion of the feedstock oil was also confirmed by conducting the FT-IR analysis, which confirms the presence of key functional groups in the biodiesel. Transesterification reaction optimization was conducted based on the RSM criteria, which identified 5.74 wt%, 63.4 °C, and 8.93:1 as optimal amount of catalyst, reaction temperature, and methanol-to-oil molar ratio, respectively. The experimental data were modeled to a quadratic polynomial, which successfully predicted the highest optimal biodiesel yield of 97.72%. The prediction was validated against the maximum actual yield of 96.38% and the experimental yield of 96.91% calculated under the predicted optimal conditions.

Future studies should be carried out on the exhaust gas emissions and performance of engines using LFW biodiesel to evaluate its environmental impact compared to conventional diesel. Additionally, research should focus on the techno-economic assessment and scaling up the proposed methodology to evaluate the process feasibility for commercial use. Finally, the by-products generated during the production process present opportunities for value-added applications that can be exploited.

Conflict of Interest

The authors declare no conflict of interest.

References

1. A Hawash, S., E. Esmail Ebrahiem, and H. A Farag, *Kinetics of esterification of oleic and linoleic free fatty acids.* Journal of Advanced Engineering Trends, 2020. **39**(1): p. 25-36 DOI: https://doi.org/10.21608/jaet.2020.73328.

2. Kylili, A., Q. Thabit, A. Nassour, and P.A. Fokaides, *Adoption of a holistic framework for innovative sustainable renewable energy development: A case study*. Energy sources, Part A: Recovery, utilization, and environmental effects, 2021: p. 1-21 DOI: https://doi.org/10.1080/15567036.2021.1904058.

3. Abdalla, E.A. and N. Abdalla, *Process Development for Conversion of Carbon Dioxide to Dimethyl Ether*. Journal of Advanced Engineering Trends, 2024. **43**(2): p. 369-383 DOI: https://doi.org/10.21608/jaet.2023.223330.1255.

4. Abdulrazak, L.F., A. Islam, and M.B. Hossain, *Towards energy sustainability: Bangladesh perspectives.* Energy Strategy Reviews, 2021. **38**: p. 100738 DOI: https://doi.org/10.1016/j.esr.2021.100738.

5. Balasubramanian, D., et al., *Numerical and experimental evaluation on the pooled effect of waste cooking oil biodiesel/diesel blends and exhaust gas recirculation in a twin-cylinder diesel engine.* Fuel, 2021. **287**: p. 119815 DOI: https://doi.org/10.1016/j.fuel.2020.119815.

6. Chakrabarti, M.H., et al., *Status of biodiesel research and development in Pakistan*. Renewable and Sustainable Energy Reviews, 2012. **16**(7): p. 4396-4405 DOI: https://doi.org/10.1016/j.rser.2012.03.064.

7. Yuliana, et al., *Utilization of waste capiz shell–Based catalyst for the conversion of leather tanning waste into biodiesel.* Journal of Environmental Chemical Engineering, 2020. **8**(4): p. 104012 DOI: https://doi.org/10.1016/j.jece.2020.104012.

8. Dagne, H., R. Karthikeyan, and S. Feleke, *Waste to energy: response surface methodology for optimization of biodiesel production from leather fleshing waste*. Journal of Energy, 2019. **2019**(1): p. 7329269.

9. Appala, V.N.S.G., N.N. Pandhare, and S. Bajpai, *Biorefining of leather solid waste to harness energy and materials—A review*. Biomass Conversion and Biorefinery, 2022 DOI: https://doi.org/10.1007/s13399-022-02455-8.

10. Abbaszaadeh, A., B. Ghobadian, M.R. Omidkhah, and G. Najafi, *Current biodiesel production technologies: A comparative review*. Energy Conversion and Management, 2012. **63**: p. 138-148 DOI: https://doi.org/10.1016/j.enconman.2012.02.027.

11. Aathika A. R, S., et al., *Enhanced biohydrogen production from leather fleshing waste co-digested with tannery treatment plant sludge using anaerobic hydrogenic batch reactor*. Energy Sources, Part A: Recovery, Utilization, and Environmental Effects, 2018. **40**(5): p. 586-593 DOI: https://doi.org/10.1080/15567036.2018.1435754.

12. Kanagaraj, J., K. Velappan, N. Babu, and S. Sadulla, *Solid wastes generation in the leather industry and its utilization for cleaner environment-A review*. 2006 DOI: https://doi.org/10.1002/chin.200649273.

13. Alptekin, E., M. Canakci, and H. Sanli, *Evaluation of leather industry wastes as a feedstock for biodiesel production.* Fuel, 2012. **95**: p. 214-220 DOI: https://doi.org/10.1016/j.fuel.2011.08.055.

14. İşler, A., S. Sundu, M. Tüter, and F. Karaosmanoğlu, *Transesterification reaction of the fat originated from solid waste of the leather industry*. Waste Management, 2010. **30**(12): p. 2631-2635 DOI: https://doi.org/10.1016/j.wasman.2010.06.005.

15. Balat, M. and H. Balat, *Progress in biodiesel processing.* Applied energy, 2010. **87**(6): p. 1815-1835 DOI: https://doi.org/10.1016/j.apenergy.2010.01.012.

16. Astm, D., *Standard specification for biodiesel fuel blend stock (B100) for middle distillate fuels.* ASTM International, West Conshohocken, 2012.

17. Ranjitha, J., S. Gokul Raghavendra, S. Vijayalakshmi, and B. Deepanraj, *Production, optimisation and engine characteristics of beef tallow biodiesel rendered from leather fleshing and slaughterhouse wastes.* Biomass Conversion and Biorefinery, 2020. **10**: p. 675-688 DOI: https://doi.org/10.1007/s13399-019-00501-6.

18. Ranjith Kumar, R., P. Hanumantha Rao, and M. Arumugam, *Lipid extraction methods from microalgae: a comprehensive review*. Frontiers in Energy Research, 2015. **2**: p. 61 DOI: https://doi.org/10.3389/fenrg.2014.00061.

19. Abdulrahman, R.K., *Sustainable biodiesel production from waste cooking oil and chicken fat as an alternative fuel for diesel engine.* Eur Sci J, 2017. **13**(10.19044) DOI: https://doi.org/10.19044/esj.2017.v13n3p235.

20. Mozhiarasi, V., T.S. Natarajan, V. Karthik, and P. Anburajan, *Potential of biofuel production from leather solid wastes: Indian scenario.* Environmental Science and Pollution Research, 2023. **30**(60): p. 125214-125237 DOI: https://doi.org/10.1007/s11356-023-28617-3.

21. Zulqarnain, et al., *A comprehensive review on oil extraction and biodiesel production technologies.* Sustainability, 2021. **13**(2): p. 788 DOI: https://doi.org/10.3390/su13020788.

22. Mustapha, A., T. Amodu, and R. Adepoju, *Effects of degumming waste cooking oil on the physicochemical and fuel properties of biodiesel.* Journal of Applied Sciences and Environmental Management, 2020. **24**(5): p. 749-753 DOI: https://doi.org/10.4314/jasem.v24i5.3.

23. Filli è res, R., B. Benjelloun ‐ Mlayah, and M. Delmas, *Ethanolysis of rapeseed oil: Quantitation of ethyl esters, mono ‐, di ‐, and triglycerides and glycerol by high ‐ performance size ‐ exclusion chromatography.* Journal of the American Oil Chemists' Society, 1995. **72**(4): p. 427-432 DOI: https://doi.org/10.1007/BF02636083.

24. Saad, M., B. Siyo, and H. Alrakkad, *Preparation and characterization of biodiesel from waste cooking oils using heterogeneous Catalyst (Cat. TS-7) based on natural zeolite.* Heliyon, 2023. **9**(6) DOI: https://doi.org/10.1016/j.heliyon.2023.e15836.

25. Modiba, E., P. Osifo, and H. Rutto, *The use of impregnated perlite as a heterogeneous catalyst for biodiesel production from marula oil.* Chemical Papers, 2014. **68**(10): p. 1341-1349 DOI: https://doi.org/10.2478/s11696-014-0583-1.

26. Erchamo, Y.S., T.T. Mamo, G.A. Workneh, and Y.S. Mekonnen, *Improved biodiesel production from waste cooking oil with mixed methanol–ethanol using enhanced eggshell-derived CaO nano-catalyst.* Scientific Reports, 2021. **11**(1): p. 6708 DOI: https://doi.org/10.1038/s41598-021-86062-z.

27. Emma, A.F., S. Alangar, and A.K. Yadav, *Extraction and characterization of coffee husk biodiesel and investigation of its effect on performance, combustion, and emission characteristics in a diesel engine*. Energy Conversion and Management: X, 2022. **14**: p. 100214 DOI: https://doi.org/10.1016/j.ecmx.2022.100214.

28. Yuliana, M., et al., *A one-pot synthesis of biodiesel from leather tanning waste using supercritical ethanol: Process optimization.* Biomass and Bioenergy, 2020. **142**: p. 105761 DOI: https://doi.org/10.1016/j.biombioe.2020.105761.